Electronic Structure of Li(Co, Mg)O_2 Studied by Electron Energy-Loss Spectrometry and First-Principles Calculation†

X. G. Xu,‡ C. Li,‡ J. X. Li,§ U. Kolb,§ F. Wu,⊥ and G. Chen*,‡

College of Materials Science and Engineering, Jilin University, Changchun, 130023, P. R. China, and State Key Laboratory of Theoretical and Computational Chemistry, Jilin University, Changchun, 130023, P. R. China, Institute of Physical Chemistry, Johaness-Gutenberg University of Mainz, D-55118 Mainz, Germany, and Beijing Institute of Technology, Beijing, 100081, P. R. China

Received: May 31, 2003; In Final Form: August 22, 2003

Electronic structures of Mg-doped $LiCoO_2$ were studied both experimentally via electron energy-loss spectroscopy (EELS) and theoretically via ab initio calculations based on density-functional theory. The Co $L_{2,3}$ edge and O K edge were employed to probe effects of Mg doping on the electronic structure of Co 3d and O 2p states. According to the EELS results, Co tends to be a mixed-valence state, and O becomes more closed-shell characteristic with Mg doping. Quantum-mechanical calculations are performed using a total-energy pseudopotential code, CASTEP. Density of states and partial density of states are calculated, which are consistent with EELS spectra. Both experimental and theoretical evidence of the change in the valence state of both Co and O are revealed. A charge balance mechanism in Mg-doped $LiCoO_2$ is suggested.

I. Introduction

A number of studies on $LiCoO_2$ have been conducted recently due to its good electrochemical performance and usage as cathode material of rechargeable lithium ion batteries. $LiCoO_2$ has high working voltage, excellent reversible Li ion intercalation, stable layer crystal structure, and long cycle stability.[1−8] Tukamoto and West[9] studied the conduction mechanism of $LiCoO_2$ and the influence of dopants on its conductivity and electrochemical performance. It was found that conductivity increases by over 2 orders of magnitude to $\sim$0.5 S cm^{-1} for a typical doped material $Li(Co_xMg_{1-x})O_2$ ($0.9 \leq x \leq 1$), which retains good electrochemical property, although there is a small reduction in capacity.[9] Tukamoto and West suggested a charge balance mechanism to explain both increase in the electronic conductivity and reduction in capacity.

Both experimental and ab initio studies were conducted on the electronic structure of $LiCoO_2$ to reveal its effect on the electrochemical property[10−16] so that the electronic structures of $LiCoO_2$ are clearly understood. To understand the effects of Mg doping on the electronic structure induced by so-called charge disproportionation,[17] we investigated the electronic structure of this Mg-doped $LiCoO_2$ experimentally and theoretically. Electron energy-loss spectroscopy (EELS) has been proven to be a valuable method to investigate the electronic structure of materials and has been employed in the study of $LiCoO_2$.[12,18] Thus, EELS was used to examine the effect of Mg doping on the electronic structure of $LiCoO_2$. Czyzyk et al. demonstrated that a one-particle band-structure approach is basically adequate for $LiCoO_2$,[13] which allows us to understand the properties of Mg-doped $LiCoO_2$ via the ab initio calculations.

We carried out this study to understand increase in the electronic conductivity based on the electronic structure.

II. Experimental and Computational Methods

Experiments. On the basis of the report from Tukamoto and West,[9] we synthesized stoichiometric single-phase $LiCoO_2$ and $Li(Co_{0.95}Mg_{0.05})O_2$ powder by using the sol−gel method. Analytical grade $Co(NO_3)_2$, $Mg(NO_3)_2$, and Li_2CO_3 were dissolved in deionized water with a cationic molar ratio of Li:(Co + Mg) = 1.05:1, citrate acid that is equal molar amounts to lithium ion was added with magnetic stirring, and the solution was heated to evaporate water until a sol was formed. The sol was heated at about 120 °C to form a gel and then was sintered for 3 h at 750 °C, yielding a dark powder. The samples were characterized by X-ray diffraction (XRD), which is taken by a Rigaku X-ray diffractometer with Cu Kα radiation (λ = 1.541 Å). Transmission electron microscope (TEM) and EELS measurements were acquired by using a Philips Tecnai F30 with acceleration voltage 300 kV and Gatan 666 parallel-detection EELS spectrometer with an energy resolution about 1.5 eV and dispersion of 0.5 eV per channel. EELS spectra were acquired in the image mode at a magnification of 340K. O K edge and Co $L_{2,3}$ edge were studied.

Calculations. All calculations were performed by the CASTEP[19] software package based on the density functional theory (DFT) in the local density approximation (LDA) through Cerius[2] graphical user interface. The electron−ion interaction is described by using an ultrasoft pseudopotential. In this scheme the pseudo-wave functions are allowed to be as soft as possible within the core region, so that the cutoff energy can be reduced dramatically. We, however, chose a cutoff energy as high as 900 eV, including a sufficient number of wave functions to get precise information about electronic structure of the crystals. Calculations started with a $R\bar{3}m$ space group. The structure of $Li(Co_{0.92}Mg_{0.08})O_2$ consists of four $LiCoO_2$ unit cells as superlattice and then having the center Co atom substituted by Mg

† Work sponsored by both Chinese National Science Foundation under Grant 50272023 and the Special Funds for Major State Basic Research Project of China under Grant 2002CB211802.

‡ Jilin University.
§ Johaness-Gutenberg University of Mainz.
⊥ Beijing Institute of Technology.
* To whom correspondence should be addressed. E-mail: jzhan@mail.jlu.edu.cn.

10.1021/jp035521y CCC: $25.00
Published on Web 09/27/2003

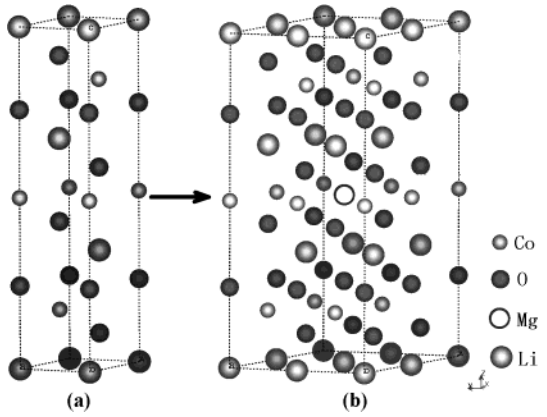

Figure 1. $LiCoO_2$ (a) and $Li(Co_{0.92}Mg_{0.08})O_2$ (b) cell for theoretical calculations.

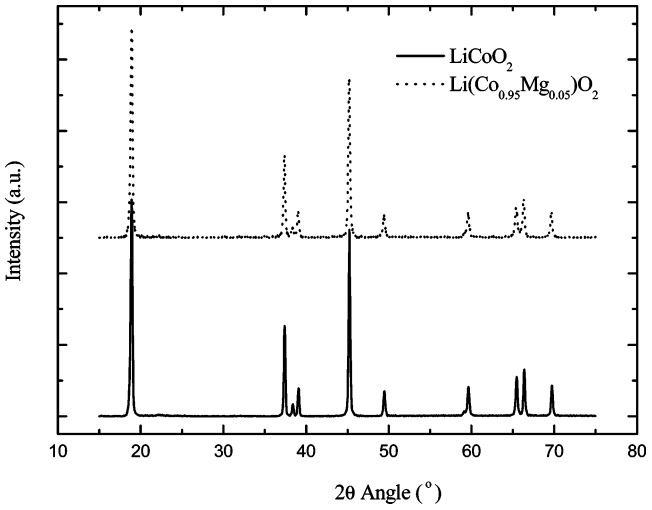

Figure 2. X-ray diffraction patterns of $LiCoO_2$ and $Li(Co_{0.95}Mg_{0.05})O_2$.

atoms as shown in Figure 1. The stoichiometry of this superlattice cell is $Li(Co_{0.92}Mg_{0.08})O_2$. The superlattice with exactly 5% Mg doping is too large and time-consuming in calculation. According to Tukamoto and West,[9] the performance of 8% Mg doping $LiCoO_2$ is almost the same as that of 5% Mg doping $LiCoO_2$. To test validity of the calculation results, we first performed a geometry optimization to minimize the system energy to calculate the structural parameters. Second, we calculated the band structure and partial density of states (PDOS) of the materials. In all these computations, 60 k-points and 16 k-points were selected for $LiCoO_2$ and Mg-doped $LiCoO_2$, respectively.

III. Results and Discussion

Both $LiCoO_2$ and $Li(Co_{0.95}Mg_{0.05})O_2$ are crystallized in a single phase $NaFeO_2$-type structure with space group $R\bar{3}m$, according to the XRD patterns shown in Figure 2. The doping of Mg ions causes an increase in the interplanar distance between the (003) basal planes, which is the effect of Coulomb repulsion between the O layers and is consistent with the tendency reported by Tukamoto and West.[9]

EELS is chosen to study the conduction bands structure. According to Graetz et al.,[12] the spectral intensity of a transition of an electron from state $|\alpha\rangle$ to the excited state $|\beta\rangle$ is given by

$$I \propto [\rho(\epsilon)/\Delta k^4]|\langle\beta|e^{-i\Delta k\cdot r}|\alpha\rangle|^2$$

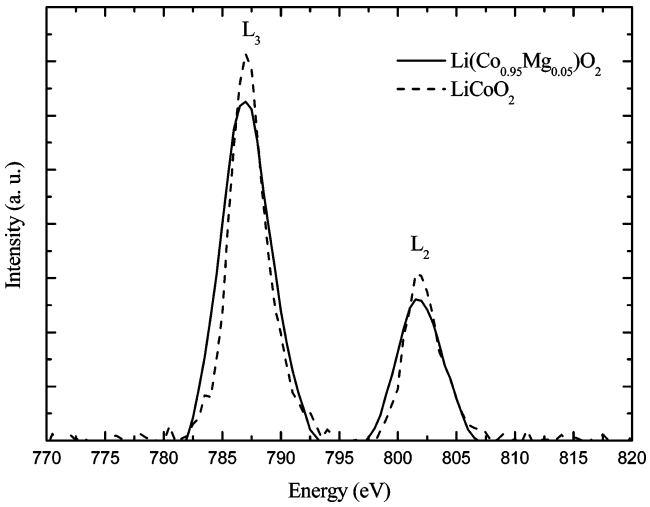

Figure 3. EELS spectra of the Co $L_{2,3}$ edge.

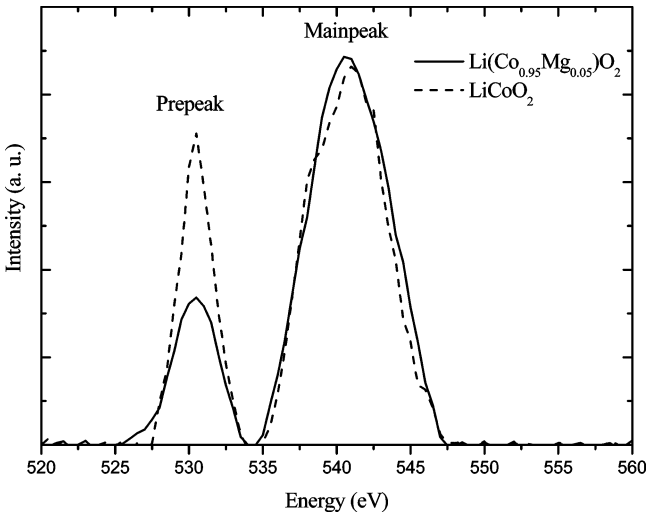

Figure 4. EELS spectra of the O K edge.

where $\rho(\epsilon)$ is the density of unoccupied states available to the excited electron.[12] Thus, the intensity of the EELS can be used to study Co 3d and O 2p bands.

The EELS results of the Co $L_{2,3}$ edge are presented in Figure 3, where solid line and dash line are the $L_{2,3}$ for $Li(Co_{0.95}Mg_{0.05})O_2$ and $LiCoO_2$, respectively. The pairs of white lines, $L_{2,3}$, come from the transitions of Co $2p_{3/2}$ and $2p_{1/2}$ core electrons, split by the spin−orbit interaction of the Co 2p core level, to an unoccupied 3d level highly hybridized with oxygen O 2p orbital, respectively. Therefore, Figure 3 reflects the state of the first unoccupied 3d band, which we will denote as e_g*. The ratio of integrated intensity, L_2/L_3, increases about 9.1% after Mg doping. Here the intensities of these two peaks are first treated by a step function according to the method given by Wang et al.[20,21] According to Wang et al., change in valence state of cations induces change in the ratio of the white lines, which enables one to identify the occupation number of 3d orbital by EELS, and a larger intensity ratio of L_2/L_3 corresponds to a higher valence state.[17] Thus, it can be concluded from the EELS results that the Mg doping increases the Co valence state, so in Mg-doped $LiCoO_2$, cobalt atoms take on a valence state between Co^{3+} and Co^{4+}.

Figure 4 shows the O K edge EELS spectra of $Li(Co_{0.95}Mg_{0.05})O_2$ (solid line) and $LiCoO_2$ (dashed line). The prepeak at 530 eV derives from the electron transition of O 1s to 2p, which reflects the occupancy of the electrons in the p shell of

TABLE 1: Experimental and Theoretical Lattices Parameters

	a			c		
	exptl (Å)	calcd (Å)	error (%)	exptl (Å)	calcd (Å)	error (%)
$LiCoO_2$	2.8167	2.838	0.8	14.006	13.862	−1.0
$Li(Co_{0.95}Mg_{0.05})O_2$	2.8199			14.014		
$Li(Co_{0.92}Mg_{0.08})O_2$		2.835			13.942	

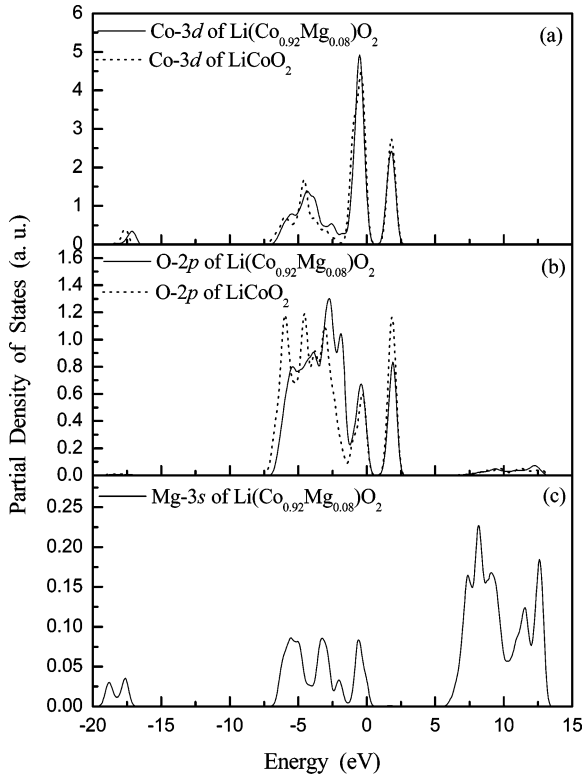

Figure 5. Calculated partial density of states: (a) Co 3d PDOS of $LiCoO_2$ and $Li(Co_{0.92}Mg_{0.08})O_2$, (b) O 2p PDOS of $LiCoO_2$ and $Li(Co_{0.92}Mg_{0.08})O_2$, and (c) Mg 3s PDOS in $Li(Co_{0.92}Mg_{0.08})O_2$.

the oxygen atoms. The main band at 541 eV comes from transition of 1s electron to the higher-energy continuum level in the crystal field. The main band remains almost unchanged with Mg doping, while the prepeak intensity decreases dramatically. According to Graetz et al.,[12] prepeak disappears in the ionic bonding oxides because the transition from 1s to 2p is prohibited due to the six electrons localized in the 2p band. Thus, the prepeak intensity is a measure of oxygen ionicity. As a result, the dramatic intensity decreasing of prepeak in Mg-doped material indicates that oxygen ions in $Li(Co_{0.95}Mg_{0.05})O_2$ have more closed-shell characteristic than in $LiCoO_2$. In other words, oxygen ions in $Li(Co_{0.95}Mg_{0.05})O_2$ are closer to the −2 valence state than in $LiCoO_2$.

The electronic structure of Mg doping material was investigated by a quantum-mechanical calculation using a total-energy pseudopotential code, CASTEP. Theoretical structural parameters are compared with the experimental data as shown in Table 1. The error of $LiCoO_2$ is within 1%, which reveals the validity of calculation that reflects the feature of the crystals. The band gap from the valence bands to the conduction bands decreases from 1.33 to 1.27 eV with Mg doping, which is not big enough to be in charge of the increase of the observed electronic conductivity.

Calculated partial density of states (PDOS) for Mg 3s, O 2p, and Co 3d are shown in Figure 5.

According to Aydinol et al.,[14] the PDOS of Co 3d in Figure 5a can be assigned to three main parts. The band from 0.7 to 2.5 eV corresponds to the unoccupied conduction bands denoted by e_g*, the band form −2 to 0.7 eV corresponds to the partially occupied valence bands, denoted by t_{2g}, and the occupied valence bands ranging from −7 to −2 eV are denoted by e_g^b. The corresponding numbers of states can be obtained by integrating the density of states of each bands which are listed in Table 2. The quantity analysis of Co atoms of these three bands in Table 2 shows that e_g*, t_{2g}, and e_g^b states change by −5.5%, −10.3%, and 20% after Mg doping, respectively, and the total density does not change within the error of calculation. Total density of states represents total number of 3d electrons in Co and is a conserved quantity. The states distribution in occupied t_{2g} and e_g^b bands and unoccupied e_g* band changes with doping and reflects the effect of Mg doping on the O 2p and Co 3d hybridization. Obviously, the introduction of Mg in $LiCoO_2$ changes Co 3d electrons distribution in different energy bands.

TABLE 2: Integration Intensity of Co 3d and O 2p PDOS in $LiCoO_2$ and $Li(Co_{0.92}Mg_{0.08})O_2$ for Different Bands

	e_g*	t_{2g}	e_g^b	total
Co[a]	2.010 53	4.747 24	2.949 45	9.707 22
Co[b]	1.898 93	4.256 78	3.544 39	9.700 11
O[a]	0.843 94	0.562 42	4.122 06	5.528 42
O[b]	0.612 48	0.634 95	4.310 96	5.558 39

[a] Atoms in $LiCoO_2$. [b] Atoms in $Li(Co_{0.92}Mg_{0.08})O_2$.

For a transition-metal ion in the octahedral symmetry,[14] the d_{z^2} and $d_{x^2-y^2}$atomic orbitals directly overlap with the p_x, p_y, and p_z orbitals of the oxygen along the octahedral directions. This σ overlap makes up the e_g^b and e_g* bands. For a strongly ionic bond, the unoccupied antibonding bands e_g* mainly consists of the metal d states, whereas the occupied bonding counterpart e_g^b is predominantly of oxygen p character. But for a covalent bond, the unoccupied e_g* band and occupied e_g^b band consists of both metal d states and oxygen p states. The bond between Co 3d and O 2p in $LiCoO_2$ shows covalent character according to the PDOS results. The remaining d_{xy}, d_{xz}, and d_{yz} orbitals point away from the oxygen and form occupied nonbonding t_{2g} bands. So the distribution of Co 3d electrons between the occupied t_{2g} and e_g^b bands indicates the electron number participating in the 3d−2p bonding. Therefore, larger density of states of e_g^b corresponds to a higher Co valence state; in the same way a lower density of states of t_{2g} corresponds to a higher Co valence state as well.

As shown in the changes in PDOS of 3d states of Co atoms (Figure 5a and Table 2), compared to those in $LiCoO_2$, both increase in the density of states of e_g^b and decrease in the density of states of t_{2g} in Mg-doped $LiCoO_2$ suggest that d electrons move from nonbonding bands to bonding bands, and more d electrons participate in the 3d−2p bonding. Correspondingly, the valence state of Co in Mg-doped $LiCoO_2$ is higher than that in $LiCoO_2$. This change of valence state is consistent with the EELS Co $L_{2,3}$ edge result.

Figure 5b is the PDOS of O. Obviously, the first conduction bands e_g* decrease dramatically with Mg doping. The states number of unoccupied e_g* reduces from 0.84 to 0.61. Correspondingly, the occupied numbers of states for t_{2g} and e_g^b

bands of O in Li($Co_{0.92}Mg_{0.08}$)O_2 increase, and the total states for O 2p is a conserved quantity. Milliken population also shows that the net charge transfer to O atom increases 0.27 e after Mg doping. The number of states of e_g* is directly related to the valence state of oxygen. For a pure ionic compound, the intensity of e_g* bands is zero, because all p orbitals are filled by electrons, which corresponds to a all-filled p valence band below the Fermi level. The lowered intensity in e_g* bands of O in Li($Co_{0.92}$-$Mg_{0.08}$)O_2 indicates that the O ion becomes more closed-shell characteristic after Mg doping and p bands in O tend to be filled as valence bands, which corresponds to the observed lowing prepeak in O K edge of EELS. The Mg 3s PDOS in Li($Co_{0.92}$-$Mg_{0.08}$)O_2 is presented in Figure 5c. There are only a few s states below the Fermi level that can be occupied by electrons, indicating that Mg is highly ionized in this compound.

Tukamoto and West[9] suggested a compensation mechanism in Mg-doped $LiCoO_2$

$$2Co^{3+} \rightarrow Mg^{2+} + Co^{4+}$$

Both ab initio calculations and EELS results show that the valence states of both Co and O change simultaneously. Charge disproportionation induced by Mg doping reflects on both Co and O. It is likely that the charge compensation mechanism can be written as

$$2Co^{3+} + O^{x-} \rightarrow Mg^{2+} + Co^{3+\delta} + O^{y-}$$

where $0 < x < y < 2$.

IV. Conclusion

The electronic structures of $LiCoO_2$ and Mg-doped $LiCoO_2$ were studied both experimentally and theoretically. The experimental result of EELS and theoretical results of CASTEP code ab initio calculation are in good agreement with each other. Both show that the Mg doping induces a mixed valences state of Co ion and a more closed-shell characteristic O ion, which gives rise to a grow in the electronic conductivity. On the basis of the experimental and theoretical electronic structure, a more complicated charge balance mechanism than that suggested by Tukamoto and West[9] is recommended.

Acknowledgment. This work was sponsored by both the Chinese National Science Foundation under Grant 50272023 and the Special Funds for Major State Basic research Project of China under Grant 2002CB211802.

References and Notes

(1) van Elp, J.; Wieland, J. L.; Eskes, H.; Kuiper, P.; Sawatzky, G. A.; de Groot, F. M. F.; Turner, T. S. *Phys. Rev. B* **1991**, *44*, 6090.
(2) Ohzuku, T.; Ueda, A. *Solid State Ionics* **1994**, *69*, 201.
(3) Chiang, Y. M.; Jang, Y. I.; Wang, H. F.; Huamg, B. Y.; Sadoway, D. R.; ye, P. X. *J. Electrochem. Soc.* **1998**, *145*, 877.
(4) Ganguly, P.; Venkatraman, T. N.; Rajanohanan, P. R.; Ganapathy, S. *J. Phys. Chem. B* **1997**, *101*, 11099.
(5) Kumta, P. N.; Gallet, D.; Waghray, A.; Blomgren, G. E.; setter, M. P. *J. Power Sources* **1998**, *72*, 91.
(6) Dahn, J. R.; Van Sacken, U.; Juzkow, M. W.; Al-Janaby, H. *J. Electrochem. Soc.* **1991**, *138*, 2207.
(7) Ohzuku, T.; Ueda, A. *J. Electrochem. Soc.* **1994**, *141*, 2972.
(8) Numata, K.; Sakaki, C.; Yamanaka, S. *Chem. Lett.* **1997**, 725.
(9) Tukamoto, H.; West, A. R. *J. Electrochem. Soc.* **1997**, *144*, 3164.
(10) Van der Ven, A.; Aydinol, M. K.; Ceder, G. *Phys. Rev. B* **1998**, *58*, 2975.
(11) Yoon, W. S.; Kim, K. B.; Kim, M. G.; Lee, M. K.; Shin, H. J.; Lee, J. M.; Lee, J. S.; Yo, C. H. *J. Phys. Chem. B* **2002**, *106*, 2526.
(12) Graetz, J.; Hightower, A.; Ahn, C. C.; Yazami, R.; Rez, P.; Fultz, B. *J. Phys. Chem. B* **2002**, *106*, 1286.
(13) Czyżyk, M. T.; Potze, R.; Sawatzky, G. A. *Phys. Rev. B* **1992**, *46*, 3729.
(14) Aydinol, M. K.; Kohan, A. F.; Ceder, G. *Phys. Rev. B* **1997**, *56*, 1354.
(15) Arroyo y de Dompablo, M. E.; Marianetti, C.; Van der Ven, A.; Ceder, G. *Phys. Rev. B* **2001**, *63*, 144107.
(16) Marianetti, C. A.; Morgan, D.; Ceder, G. *Phys. Rev. B* **2001**, *63*, 224304.
(17) Wang, Z. L.; Kang, Z. C. *Functional and Smart Materials Structural Evolution and Structure Analysis*; Plenum: New York, 1998.
(18) Köstlmeier, S.; Elsässer, C. *Phys. Rev. B* **1999**, *60*, 14025.
(19) Payne, M. C.; Teter, M. P.; Allan, D. C.; Arias, T. A.; Joannopoulos, J. D. *Rev. Mod. Phys.* **1992**, *64*, 1045.
(20) Wang, Z. L.; Yin, J. S.; Jiang, Y. D. *Micron* **2000**, *31*, 571.
(21) Wang, Z. L.; Bentley, J.; Evans, N. D. *Micron* **2000**, *31*, 355.